Local Analysis for 3D Reconstruction of Specular Surfaces – Part II

Silvio Savarese and Pietro Perona

California Institute of Technology, Pasadena CA 91200, USA

Abstract. We analyze the problem of recovering the shape of a mirror surface. We generalize the results of [1], where the special case of planar and spherical mirror surfaces was considered, extending that analysis to any smooth surface. A calibrated scene composed of lines passing through a point is assumed. The lines are reflected by the mirror surface onto the image plane of a calibrated camera, where the intersection and orientation of such reflections are measured. The relationship between the local geometry of the surface around the point of reflection and the measurements is analyzed. We give necessary and sufficient conditions, as well as a practical algorithm, for recovering first order local information (positions and normals) when three intersecting lines are visible. A small number of 'ghost solutions' may arise. Second order surface geometry may also be obtained up to one unknown parameter. Experimental results with real mirror surfaces are presented.

Keywords: Shape recovery, geometry, mirror surfaces.

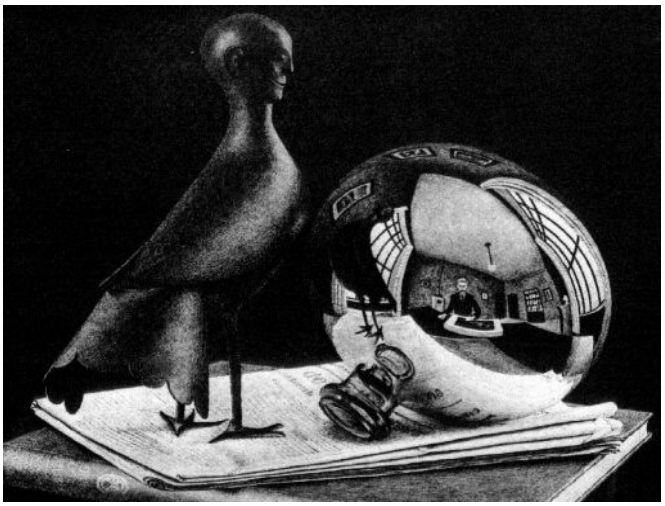

Fig. 1. M.C. Escher (1935): Still Life with Spherical Mirror

1 Introduction and Motivation

We are interested in the possibility of recovering information on the shape of a surface from the specular component of its reflectance function. Since we wish to ignore the contributions of shading and texture, we will study surfaces that are perfect mirrors. A curved mirror surface produces 'distorted' images of the surrounding world. For example, the image of a straight line reflected by a curved mirror is, in general, a curve (see Fig. 1). It is clear that such distortions are systematically related to the shape of the surface. Is it possible to invert this map, and recover the shape of the mirror from the images it reflects? The general 'inverse mirror' problem is clearly underconstrained: by opportune manipulations of the surrounding world we may produce almost *any* image from *any* curved mirror surface as illustrated by the anamorphic images that were popular during the Renaissance. The purpose of this paper is to continue the investigation started in our previous work [1] where we presented a novel study on the basic geometrical principles linking the shape of a mirror surface to the distortions it produces on a scene. We assumed a calibrated world composed of the simplest primary structures: one point and one or more lines through it. We studied the relationship between the local geometry of the mirror surface around the point of reflection, and the position, orientation and curvature of the reflected images of such point and lines. Additionally, we derived an explicit solution for planar and spherical surfaces. In this paper we extend this analysis to generic smooth surfaces. We show that it is possible to recover first order local information (positions and normals) when three intersecting lines are reflected by the surface, although a small number of "ghost" solutions in the reconstruction may arise. Such solutions might be removed by considering either more than 3 no-coplanar lines or a rough a priori estimate of the surface point location or a second order local differential analysis as derived in [1]. Second order surface geometry may also be obtained up to one unknown parameter, which we prove cannot be recovered from first order local measurements (position and tangents).

Applications of our work include recovering the global shape of highly glossy surfaces. Two possible situations are: a) placing a suitable calibrated pattern of intersecting lines near the specular surface and applying our analysis at the locus of the observed reflections of the pattern intersections; b) placing a calibrated reference plane near the specular surface, projecting a suitable pattern with a calibrated LCD projector over the specular surface and applying our analysis at the locus of the intersections reflected by the surface over the reference plane and observed by the camera [14]; such setup is appealing since it requires the same hardware used by common structured lighting techniques. Finally our work may provide useful mathematical tools for the analysis and the calibration of omniview cameras with curved surfaces mirrors.

A summary of the notation and results obtained in [1] is presented in Sec. 2. Main geometrical properties and the reconstruction method for general mirror surfaces are described in Sec. 3. Experimental results with real mirror surface are shown in Sec. 4. The paper is concluded with a discussion on our findings and a number of issues for further research.

1.1 Previous Work

Previous authors have used highlights as a cue to infer information about the geometry of a specular surface. Koenderink and van Doorn [10] qualitatively described how pattern of specularities change under viewer motion. This analysis was extended by Blake *et al.* and incorporated in a stereoscopic vision framework [4] [3]. Additionally, Zisserman *et al.* [13] investigated what geometrical information can be obtained from tracked motion of specularities. Other approaches were based on mathematical models of specular reflections (e.g. reflectance maps) [8] or extension of photometric stereo models [9]. Oren and Nayar developed in [11] an analysis on classification of real and virtual features and an algorithm recovering the 3D surface profiles traveled by virtual features. Zheng and Murata developed a system [12] where extended lights illuminate a rotating specular object whose surface is reconstructed by analyzing the motion of the highlight stripes. In [7], Halsead *et al.* proposed a reconstruction algorithm where a surface global model is fitted to a set of normals by imaging a pattern of light reflected by specular surface. Their results were applied in the interactive visualization of the cornea. Finally, Perard [14] used a structured ligthing technique for the iterative reconstruction of surface normal vectors and topography.

Contrary to previous techniques, in our method, surrounding word and viewer are assumed to be static. Monocular images rather than stereo pairs are needed for the reconstruction. The analysis is local and differential rather than global and algebraic.

2 The geometry of the specular reflections

Our goal is to obtain local geometrical information about an unknown smooth mirror surface. The basic geometric setup is depicted in Fig. 2 (left panel). A calibrated pattern is reflected by a curved mirror surface and the reflection is observed by a calibrated camera. The pattern may be formed by either one point or one point and one line, or 2 (or more) intersecting lines. We start our analysis studying which local information about the surface can be obtained by considering a single pattern point and its corresponding image reflection. We begin with a summary of notation and results in [1].

2.1 Definitions and basic specular reflection constraints

A point (or a vector) in the 3D space is expressed by a column 3-vector and is denoted by a bold letter (e.g. $\mathbf{x} = (x\, y\, z)^T$). A vector whose norm is 1 is denoted by a bold letter with hat (e.g. $\hat{\mathbf{n}}$). A coordinate reference system $[XYZ]$ is chosen with origin $\mathbf{O}_c$ in the center of projection of the camera. See Fig. 2 (right panel). Let $\mathbf{x}_p$ be the pattern point. $\mathbf{x}_i$ denotes the image of $\mathbf{x}_p$ reflected by the surface and $\mathbf{x}_m$ denotes the corresponding reflection point on the mirror surface. Since the camera and pattern are calibrated, $\mathbf{x}_p$ and $\mathbf{x}_i$ are known, whereas $\mathbf{x}_m$ is unknown. The normal to the surface in $\mathbf{x}_m$ is indicated by $\hat{\mathbf{n}}_m$ and is unknown

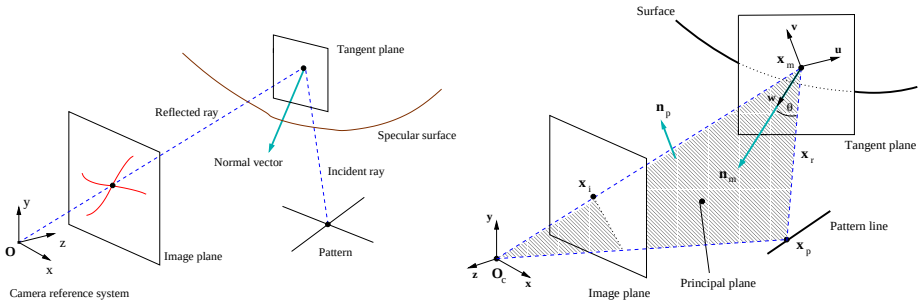

Fig. 2. Left panel: the basic setup. **Right panel**: the geometry

as well. Let us call *principal plane* the plane defined by $\mathbf{x}_i$, $\mathbf{x}_p$ and $\mathbf{O}_c$ (dashed area in Fig. 2 – right panel) and let $\hat{\mathbf{n}}_p$ be its normal vector. Hence $\hat{\mathbf{n}}_p$ is a known quantity. The geometry of our setup satisfies 3 basic constraints: **1**) The perspective projection constraint: the point $\mathbf{x}_m$ must belong to the line defined by $\mathbf{O}_c$ and $\mathbf{x}_i$, namely,

$$\mathbf{x}_m = s\hat{\mathbf{x}}_i \tag{1}$$

where s is the distance between the center of the camera $\mathbf{O}_c$ and $\mathbf{x}_m$. As a result, $\mathbf{x}_m$ is known up to a scalar factor. **2**) The incident vector $\mathbf{x}_m - \mathbf{x}_p$ and the reflected vector $\mathbf{x}_m - \mathbf{O}_c$ must belong to the same plane, that is, the principal plane. **3**) The angle between incident vector and normal vector must be equal to the angle between reflected vector and normal vector. By combining such constraints it is straightforward to conclude that $\mathbf{n}_m$ and reflection angle θ are parametrized by s as follows:

$$\mathbf{n}_m = [\hat{\mathbf{x}}_i - \frac{(s\hat{\mathbf{x}}_i - \mathbf{x}_p)}{\|s\hat{\mathbf{x}}_i - \mathbf{x}_p\|}] \times \hat{\mathbf{n}}_p \tag{2}$$

$$\cos\theta = \frac{\sqrt{2}}{2}\sqrt{\frac{s - \hat{\mathbf{x}}_i^T\mathbf{x}_p}{\|s\hat{\mathbf{x}}_i - \mathbf{x}_p\|} + 1} \tag{3}$$

See [1] for a derivation of these equations.

2.2 The pattern line constraint

Since our goal is to obtain local geometrical information about the mirror surface at the reflection point $\mathbf{x}_m$, as first attempt, we would like to compute the unknown parameter s. We notice that, if s were known, by means of Eq. 1 and Eq. 2, the surface point $\mathbf{x}_m$ and the surface normal vector $\hat{\mathbf{n}}_m$ would be known as well. Thus, as to the first order surface description, the local geometry would be fully recovered. It is clear that a further constraint is needed. To this end, we consider one pattern line through $\mathbf{x}_p$. The pattern line reflected by the mirror surface can be be captured by the camera and the tangent direction of such

observed curve at $\mathbf{x}_i$ can be measured. Before investigating how to exploit such measurement we first introduce further geometrical objects.

A more suitable coordinate reference system $[UVW]$, which we call *principal reference system* (see Fig. 2 – right panel) was first introduced by Blake in [3]. The principal reference system is centered in $\mathbf{x}_m$; the $\hat{\mathbf{w}}$ axis is coincident with $\hat{\mathbf{n}}_m(s)$; the $\hat{\mathbf{v}}$ axis is coincident with $\hat{\mathbf{n}}_p$; the $\hat{\mathbf{u}}$ axis is given by $\hat{\mathbf{u}} = \hat{\mathbf{v}} \times \hat{\mathbf{w}}$. Thus, a point $\mathbf{x}$ in the $[XYZ]$ and the corresponding point $\mathbf{x}'$ in $[UVW]$ are related by transformation $\mathbf{x}' = \mathbf{R}^T(\mathbf{x} - \mathbf{T})$, where $\mathbf{R}(s) = [\, \hat{\mathbf{n}}_p \times \hat{\mathbf{n}}_m(s) \quad \hat{\mathbf{n}}_p \quad \hat{\mathbf{n}}_m(s) \,]$ and $\mathbf{T}(s) = s\hat{\mathbf{x}}_i$. For instance, the center of the camera becomes $-\mathbf{R}(s)^T\ \mathbf{T}(s)$. Notice that the transformation is function of s. From now on, we shall always omit s from the notation (unless we need to show explicitly such dependency) and assume that we work in the principal reference system.

The pattern is formed by one point and one line passing through it. Let $\mathbf{x}_{po}$ be such a point and $\mathbf{\Delta p} = [\Delta p_u\ \Delta p_v\ \Delta p_w]^T$ the orientation vector of the line in space. We can describe the generic pattern line in parametric form as follows:

$$\mathbf{x}_p(t) = \mathbf{x}_{po} + t\mathbf{\Delta p} \tag{4}$$

where t is a parameter. Since the pattern is calibrated, $\mathbf{x}_{po}$ and $\mathbf{\Delta p}$ are known quantities in the $[XYZ]$ reference system, whereas they become function of s in the $[UVW]$ reference system.

In general, the mirror surface can be implicitly described by an equation $g(x, y, z) = 0$. Since we are interested in analyzing the surface locally, we can consider the corresponding *Monge representation* of the surface; that is, the surface can be described by the graph $z = G(x, y)$. In the principal reference system, the normal of the surface at the origin is $\hat{\mathbf{w}}$ and the tangent plane to the surface at the origin is the plane defined by $\hat{\mathbf{u}}$ and $\hat{\mathbf{v}}$. Therefore the equation of the surface around $\mathbf{x}_m$ can be written in the *special Monge form* [6] as follows:

$$w = \frac{1}{2!}(au^2 + 2cuv + bv^2) + \frac{1}{3!}(eu^3 + 3fu^2v + 3guv^2 + hv^3) + \cdots \tag{5}$$

Notice that the parameters a, b, c, $\cdots$ of the Monge form are unknown, since we do not have any information about the mirror surface.

Let us define a mapping function $\mathbf{f}$ which maps a point $\mathbf{x}_p$ (within the pattern line) into the corresponding reflection point $\mathbf{x}_m$ in the mirror surface, given a fixed observer $\mathbf{O}_c$. Since $\mathbf{x}_p$ is constrained to belong to the parametrized pattern line, the mapping can be expressed as follows:

$$\mathbf{f} : t \in \Re \rightarrow \mathbf{x}_m \in \Re^3 \tag{6}$$

In other words, Eq. 6 defines a parametrized space curve $\mathbf{f}(t)$ lying within the mirror surface which describes the position of the reflection point $\mathbf{x}_m$, as t varies. When $t = t_o = 0$, $\mathbf{x}_m = \mathbf{x}_{m_o} = \mathbf{f}(t_o)$, namely, the origin of the principal reference system. The pattern line, reflected by the mirror surface, is imaged as a curve line in the image plane. We call such curve $\mathbf{f}_i(t)$. $\mathbf{f}_i(t)$ is essentially the perspective projection of $\mathbf{f}(t)$ onto the image plane. Let $\mathbf{x}_{io}$ be the perspective projection of

$\mathbf{x}_{m_o}$ onto the image plane. Let $\mathbf{t}_o = [\dot{u}_o \ \dot{v}_o \ \dot{w}_o]^T$ and $\mathbf{t}_{io}$ be the tangent vectors of the curves $\mathbf{f}(t)$ and $\mathbf{f}_i(t)$ at t_o respectively.

It is not difficult to show (see [1]) that $\hat{\mathbf{t}}_{io}$ and $\hat{\mathbf{t}}_o$ are linked by the following relationship:

$$\hat{\mathbf{t}}_o = \frac{\hat{\mathbf{n}}_m \times (\hat{\mathbf{O}}_c \times \hat{\mathbf{t}}_{io})}{\|\hat{\mathbf{n}}_m \times (\hat{\mathbf{O}}_c \times \hat{\mathbf{t}}_{io})\|} \tag{7}$$

Thus, since $\hat{\mathbf{t}}_{io}$ can be measured, $\hat{\mathbf{t}}_o$ turns out to be known, up to s.

We present now the fundamental relationship between $\hat{\mathbf{t}}_o$, the geometry of the pattern line, the center of the camera $\mathbf{O}_c$, the reflection point $\mathbf{x}_{m_o}$ and the parameters of the Taylor expansion of the surface Monge form G. Introducing the problem as Chen and Arvo did in [5] and following the analysis described in [1], we obtain:

$$\tan\varphi = \frac{(J_u - 2a\cos\theta)B_v + 2cB_u\cos\theta}{(J_v - 2b\cos\theta)B_u + 2cB_v\cos\theta} \tag{8}$$

where,

$$\begin{array}{lll} B_v = -\frac{\Delta p_v}{\|\mathbf{x}_{po}\|} & B_u = \frac{1}{\|\mathbf{x}_{po}\|}(\Delta p_w \cos\theta \sin\theta - \Delta p_u \cos^2\theta) & \\ J_u = \cos^2\theta \, \frac{s+\|\mathbf{x}_{po}\|}{s\,\|\mathbf{x}_{po}\|} & J_v = \frac{s+\|\mathbf{x}_{po}\|}{s\,\|\mathbf{x}_{po}\|} & \tan\varphi = \frac{\dot{v}_o}{\dot{u}_o} \end{array} \tag{9}$$

Notice that θ, $\|\mathbf{x}_{po}\|$, $\mathbf{\Delta p} = [\Delta p_u \Delta p_v \Delta p_w]^T$ depend upon s; the angle φ (namely, the orientation of $\hat{\mathbf{t}}_o$ in the surface tangent plane at $\mathbf{x}_{mo}$) can be expressed as function of s and $\hat{\mathbf{t}}_{io}$ by means of Eq. 7; a, b and c are second order parameters of the Taylor expansion of the surface Monge form (Eq. 5). Also, notice that no third and higher parameters of the Taylor expansion do appear in Eq. 8. Finally, we highlight that no assumption on the type of surface have been made, namely, Eq. 7 is valid for both concave or convex surfaces.

As a conclusion, Eq. 8 represents the constraint introduced by one pattern line passing through $\mathbf{x}_{po}$ and the tangent vector measurement $\hat{\mathbf{t}}_{io}$. However, since in Eq. 8 there appear four unknowns (s, a, b, c) rather than just s, the reconstruction problem must be solved by jointly estimating both first and second order parameters and by using more than one pattern line.

3 Recovery of the surface

As shown in [1], in the case of spherical mirror surface, we carried out an explicit solution for the distance s and the sphere curvature by means of Eq. 8 and by imposing that $a = b$ and $c = 0$. In the following sections we investigate the more general case when s, a, b, c are fully unknown. In Sec. 3.1 and 3.2, we assume that s is known and we analyze geometrical properties of the second order surface parameters. In Sec. 3.3 we explicitly describe how to estimate s.

3.1 Analysis of second order surface parameters

Let us assume that the distance s is known. As shown in Sec. 2.1, $\mathbf{x}_{mo}$, the surface tangent plane and surface normal at $\mathbf{x}_{mo}$ become known as well. As a result, the first order local description of the mirror surface is completely known if s, $\hat{\mathbf{x}}_{io}$, $\mathbf{x}_{p_o}$ and $\mathbf{O}_c$ are known. In such a case we say that the *first order description* of the mirror surface is given by the quadruplet ($\mathbf{x}_{p_o}$, $\mathbf{O}_c$, $\hat{\mathbf{x}}_{io}$, s). Thus, we want to address the following question: given a surface whose first order description is given by a quadruplet ($\mathbf{x}_{p_o}$, $\mathbf{O}_c$, $\hat{\mathbf{x}}_{io}$, s), what can we tell about the second order surface parameters a, b and c?

Let us consider n pattern lines $\lambda_1, \lambda_2, \cdots \lambda_n$ intersecting in $\mathbf{x}_{po}$. Each pattern line produces a reflected curve on the mirror surface and a corresponding tangent vector at $\mathbf{x}_{mo}$. We can impose the constraint expressed by Eq. 8 for each pattern line, obtaining the following system:

$$\begin{cases} \tan\varphi_1 = \frac{(J_u - 2a\cos\theta)B_{v_1} + 2cB_{u_1}\cos\theta}{(J_v - 2b\cos\theta)B_{u_1} + 2cB_{v_1}\cos\theta} \\ \vdots \\ \tan\varphi_n = \frac{(J_u - 2a\cos\theta)B_{v_n} + 2cB_{u_n}\cos\theta}{(J_v - 2b\cos\theta)B_{u_n} + 2cB_{v_n}\cos\theta} \end{cases} \tag{10}$$

where the subscripts $1, \cdots n$ indicate the quantities attached to $\lambda_1, \cdots \lambda_n$ respectively. After simple manipulations, we have:

$$\begin{cases} (J_u - 2a\cos\theta)B_{v_1} - (J_v - 2b\cos\theta)B_{u_1}\tan\varphi_1 + 2c\cos\theta(B_{u_1} - B_{v_1}\tan\varphi_1) = 0 \\ \vdots \\ (J_u - 2a\cos\theta)B_{v_n} - (J_v - 2b\cos\theta)B_{u_n}\tan\varphi_n + 2c\cos\theta(B_{u_n} - B_{v_n}\tan\varphi_n) = 0 \end{cases} \tag{11}$$

which is a linear system of n equations in 3 unknowns (a, b and c). The system of Eq. 11 can be expressed in the following matrix form:

$$\mathbf{H}\,\mathbf{g} = \begin{bmatrix} B_{v_1} & -B_{u_1}\tan\varphi_1 & B_{u_1} - B_{v_1}\tan\varphi_1 \\ B_{v_2} & -B_{u_2}\tan\varphi_2 & B_{u_2} - B_{v_2}\tan\varphi_2 \\ \vdots & \vdots & \vdots \\ B_{v_n} & -B_{u_n}\tan\varphi_n & B_{u_n} - B_{v_n}\tan\varphi_n \end{bmatrix} \begin{bmatrix} \alpha \\ \beta \\ \gamma \end{bmatrix} = 0 \tag{12}$$

where $\alpha = J_u - 2a\cos\theta$, $\beta = J_v - 2b\cos\theta$, $\gamma = 2c\cos\theta$, $\mathbf{H}$ and $\mathbf{g}$ are a $n \times 3$ matrix and a vector respectively capturing the quantities at right side of the equality. Eq. 12 is an homogeneous linear system in the unknowns α, β and γ. We want to study the properties of such a system.

Definition 1. *A surface, whose first order description is given by the quadruplet ($\mathbf{x}_{p_o}$, $\mathbf{O}_c$, $\hat{\mathbf{x}}_{io}$, s), is called* singular *at $\mathbf{x}_{m_o}$ if its second order parameters a,b and c are:*

$$\begin{cases} a = \frac{J_u}{2\cos\theta} \\ b = \frac{J_v}{2\cos\theta} \\ c = (\frac{J_u}{2\cos\theta} - a)(\frac{J_v}{2\cos\theta} - b) = 0 \end{cases} \tag{13}$$

As shown in details in [1], for a surface singular at $\mathbf{x}_{m_o}$, it turns out that the Jacobian attached to mapping $t_o \in \Re \rightarrow \mathbf{x}_{mo} \in \Re^3$ is singular and the resulting Eq. 8 is no longer valid.

Proposition 1. *Let us assume to have a mirror surface whose first order description is given by the quadruplet ($\mathbf{x}_{p_o}$, $\mathbf{O}_c$, $\hat{\mathbf{x}}_{io}$, s) and which is non singular at $\mathbf{x}_{m_o}$. Let us consider $n \geq 2$ pattern lines passing through $\mathbf{x}_{p_o}$ but not lying in the principal plane. Then the rank of matrix $\mathbf{H}$ is 2.*

Proof. That $\mathbf{H}$ must have rank ≤ 3 is trivial. We want to prove, by contradiction, that the rank cannot be neither 3, nor 1, nor 0. For reason of space we omit the proof of the last 2 cases. Interested readers may find more details in a forthcoming technical report. Let us suppose that $\mathbf{H}$ has rank 3. The homogeneous system of Eq. 12 has a unique solution, which must be $\mathbf{g} = 0$. Thus, $J_u - 2a\cos\theta = 0$, $J_v - 2b\cos\theta = 0$ and $2c\cos\theta = 0$. Since J_u, J_v and $\cos\theta$ are positive quantities, the surface must be singular at $\mathbf{x}_{m_o}$. As a conclusion $\mathbf{H}$ cannot be a full rank matrix. □

Proposition 1 tells us that, no matter how many tangent vector measurement $\hat{\mathbf{t}}_{io}$'s are used, the second order surface parameters a, b and c can be estimated only up to an unknown parameter. As final remark, we notice that both hypotheses of proposition 1 are necessary for observations (measured tangent vectors) to be meaningful and, therefore, for the reconstruction to be feasible. Thus, in all practical cases, both hypotheses are always satisfied and therefore the proposition verified.

Let us consider a mirror surface whose first order description is given by a quadruplet ($\mathbf{x}_{p_o}$, $\mathbf{O}_c$, $\hat{\mathbf{x}}_{io}$, s). Since rank($\mathbf{H}$)= 2, the space spanned by the rows of $\mathbf{H}$ is a plane. The vector $\mathbf{g}$ must be orthogonal to such a plane. Let $\mathbf{h_i}$ and $\mathbf{h_j}$ be any two row vectors of $\mathbf{H}$. If we define the vector $\mathbf{v} = [v_1 \ v_2 \ v_3]^T$ as follows:

$$\mathbf{v} = \mathbf{h_i} \times \mathbf{h_j} = \begin{bmatrix} -B_{u_i}\tan\varphi_i(B_{u_i} - B_{v_j}\tan\varphi_j) + (B_{u_j} - B_{v_i}\tan\varphi_i)B_{u_i}\tan\varphi_j \\ (B_{u_j} - B_{v_i}\tan\varphi_i)B_{v_j} - (B_{u_i} - B_{v_j}\tan\varphi_j)B_{v_i} \\ -B_{v_i}B_{u_j}\tan\varphi_j + B_{u_i}B_{v_j}\tan\varphi_i \end{bmatrix} \tag{14}$$

we have:

$$k\ \mathbf{v} = \mathbf{g} = \begin{bmatrix} J_u - 2a\cos\theta \\ J_v - 2b\cos\theta \\ 2c\cos\theta \end{bmatrix} \tag{15}$$

where k is a scalar. Combining Eq. 14 with Eq. 15:

$$\begin{cases} a = \frac{J_u}{2\cos\theta} - k\frac{v_1}{2\cos\theta} \\ b = \frac{J_v}{2\cos\theta} - k\frac{v_2}{2\cos\theta} \\ c = k\frac{v_3}{2\cos\theta} \end{cases} \tag{16}$$

As a result, any two tangent vector measurements suffice to constrain the second order description of the mirror surface around $\mathbf{x}_{m_o}$ up to the unknown

parameter k. Proposition 1 guarantees that we cannot do better than so, even using more than two pattern lines. Eqs. 16 give a quantitative relationship between the second order surface parameters a, b and c, any two pattern line orientations (embedded in the B_u's and B_v's), the corresponding tangent vector measurements (embedded in the φ's) and the unknown parameter k.

3.2 The space of paraboloids

In this section we introduce a $\Re^3$-space, called *space of paraboloids*, in which the geometry describing our results can be represented in a more clear fashion. In the space of paraboloids, the coordinates of a point $[a\ b\ c]^T$ univocally describe a paraboloid given by $w = au^2 + bv^2 + 2cuv$. See Fig. 3 (left panel).

Let us consider a mirror surface M^* whose first order description is given by the quadruplet $(\mathbf{x}_{p_o},\ \mathbf{O}_c,\ \hat{\mathbf{x}}_{io},\ s^*)$. Since the second order terms of the Taylor expansion around $\mathbf{x}_{m_o}$ of the surface Monge form attached to M^* define a paraboloid with parameters a, b and c, we say that the *second order description* of M^* is given by a point $\mathbf{p}$ in the space of paraboloids $\wp$. Thus, $\wp$ represents the space of all possible second order descriptions of a surface having vertex in $\mathbf{x}_{m_o}$ and normal $\mathbf{n}_{m_o}$ at $\mathbf{x}_{m_o}$. Let $\mathbf{p}^*$ be the unknown paraboloid defining the second order description of M^*. If we take n pattern lines and the corresponding tangent vector measurements in the image plane, Proposition 1 tells us that we cannot fully estimate $\mathbf{p}^*$. However, by means of Eqs. 16, with any 2 pattern lines and the corresponding measurements we can estimate a *family* of paraboloids parametrized by k. In $\wp$, such a family is a line γ described by the following parametric form:

$$\mathbf{p}(k) = \mathbf{p}_o + k\,\mathbf{v}' = \begin{bmatrix} \frac{J_u}{2\cos\theta} \\ \frac{J_v}{2\cos\theta} \\ 0 \end{bmatrix} + k\frac{\mathbf{v}}{2\cos\theta} \tag{17}$$

Proposition 2. *Consider a mirror surface M^* whose first order description is given by the quadruplet $(\mathbf{x}_{p_o},\ \mathbf{O}_c,\ \hat{\mathbf{x}}_{io},\ s^*)$ and whose second order description is given by $\mathbf{p}^*$. Assume that M^* is not singular at $\mathbf{x}_{mo}$. Then any pair of pattern lines and corresponding measurements produce the same family of paraboloids, namely, the same line γ.*

Proof. γ is constrained to pass through $\mathbf{p}_o$, which only depends on the quadruplet $(\mathbf{x}_{p_o},\ \mathbf{O}_c,\ \hat{\mathbf{x}}_{io},\ s^*)$. Additionally , γ is constrained to pass through $\mathbf{p}^*$. On the other hand, $\mathbf{p}_o$ is the second order description of a surface singular at $\mathbf{x}_{mo}$. Thus, $\mathbf{p}_o \neq \mathbf{p}^*$. As a result, γ must be invariant, no matter which pair of pattern lines and corresponding measurements are considered. □

Consider now a family of mirror surfaces whose first order description is given by the quadruplet $(\mathbf{x}_{p_o},\ \mathbf{O}_c,\ \hat{\mathbf{x}}_{io},\ s^*)$ and whose second order description is given by any paraboloid belonging to a line γ. Then, given an arbitrary pattern line, any surface belonging to the family must produce the same measurement, i.e.

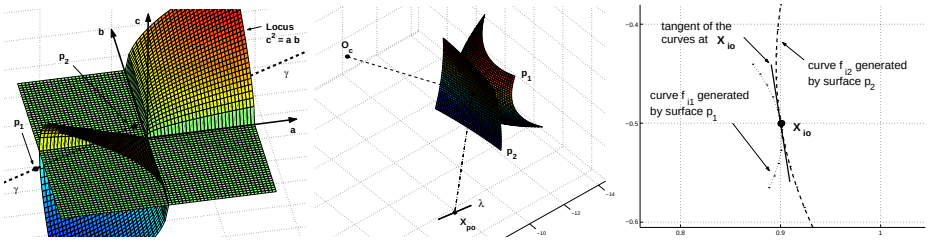

Fig. 3. Left panel: the space of paraboloids. $\mathbf{p}_1$ and $\mathbf{p}_2$ are two paraboloids belonging to the same family γ. The locus $c^2 = ab$ (namely, the set of all parabolic paraboloids) separates the space into two regions. All of the points such that $c^2 < ab$ correspond to elliptic paraboloids whereas all of points such that $c^2 > ab$ corresponds to hyperbolic paraboloids. Thus, $\mathbf{p}_1$ is elliptic whereas $\mathbf{p}_2$ is hyperbolic. **Middle panel**: $\mathbf{p}_1$ and $\mathbf{p}_2$ in the $[XYZ]$ reference system. λ is a possible pattern line. **Right panel**: Images of the reflected pattern line λ. $\mathbf{f}_{i1}$ and $\mathbf{f}_{i2}$ are generated by $\mathbf{p}_1$ and $\mathbf{p}_2$ respectively. Notice that the tangents of the curves at $\mathbf{x}_{io}$ are coincident (ambiguity of type I).

the same tangent vector $\hat{\mathbf{t}}_{io}$. This conclusion highlights a fundamental ambiguity as far as the second order description of a surface is concerned:

Proposition 3. ***Specular reflection ambiguity of type I****. Given a camera and a pattern line passing through a point $\mathbf{x}_{p_o}$, there exists a whole family of mirror surfaces producing a family of reflected image curves whose tangent vector at $\mathbf{x}_{i_o}$ is invariant — $\mathbf{x}_{i_o}$ being the image of the reflection of $\mathbf{x}_{p_o}$.*

In order to validate our theoretical results, we have implemented a program in MatLab to simulate specular reflections. Given a pattern line, a known surface (defined as a graph) and the observer, the routine computes the corresponding reflected curve imaged by the observer. In Fig. 3 an example of ambiguity of type I is provided.

3.3 Estimation of the distance parameter s

A crucial assumption made in the previous sections was that a quadruplet ($\mathbf{x}_{p_o}$, $\mathbf{O}_c$, $\hat{\mathbf{x}}_{io}$, s^*) giving the first order description of an unknown mirror surface M^* was available. However, while $\mathbf{x}_{p_o}$, $\mathbf{O}_c$, $\hat{\mathbf{x}}_{io}$ are known since we assume that both camera and pattern are calibrated, the parameter s^* still needs to be estimated, s^* being the distance between $\mathbf{O}_c$ and $\mathbf{x}_{m_o}$.

Let us take n pattern lines λ_1, λ_2, $\cdots$ λ_n intersecting in $\mathbf{x}_{po}$ and the corresponding tangent vector measurements and consider the matrix $\mathbf{H}$ of Eq. 12. Since each entry of $\mathbf{H}$ is parametrized by s, $\det(\mathbf{H}^T\mathbf{H})$ is a function of s. Let us call it $\Psi(s)$. When $s = s^*$, Proposition 1 is verified. Thus $\Psi(s^*) = 0$. On the other hand, when $s \neq s^*$, we cannot say anything about $\det(\mathbf{H}^T\mathbf{H})$ but we would expect it to be different from zero since our measurements would not be consistent with tangent vectors produced by the geometry attached to $s \neq s^*$.

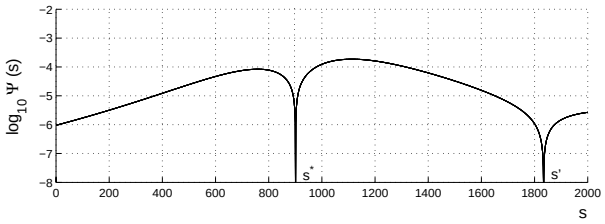

Fig. 4. An instance of $det(\mathbf{H}) = \Psi(s)$.

In Fig. 4 an instance of $\Psi(s)$ is shown. Such a plot was obtained by means of our specular reflection simulator. A triplet of pattern lines with the 3 corresponding measurements was considered. Thus, Ψ is just the determinant of the corresponding 3×3 matrix $\mathbf{H}$. As we can see from the plot, $\Psi(s)$ vanishes in s^*. However, $\Psi(s)$ vanishes in other point, s', as well. Such value of s corresponds to a wrong (or *ghost*) solution. Namely, the quadruplet ($\mathbf{x}_{p_o}$, $\mathbf{O}_c$, $\hat{\mathbf{x}}_{io}$, s') gives a first order description of a mirror surface $M' \neq M^*$ and, as far as the 3 tangent vector measurements are concerned, there is no way to discriminate such surface from the correct one. In other words, the 3 tangent vectors produced in the image plane by M^* and M' are exactly the same. This is what we call the ***specular reflection ambiguity of type II***. In our experience, only a few (usually 1 or 2, even none) ambiguities arise for each s^* (see Fig. 8).

We can think about three possible ways to get rid of such ambiguities. i) Our simulations show that the specular reflection ambiguity of type II is actually related to a particular triplet of pattern lines. Namely, by considering $m > 3$ no-coplanar pattern lines, the actual s^* can be found without ambiguities, since $\det(\mathbf{H}^T\mathbf{H})$ — the matrix $\mathbf{H}$ being $m \times 3$ — vanishes only in s^*. Further work is needed to theoretically validate such conclusions. ii) If a rough estimate of the distance is available, then usually only one solution is consistent with this estimate. iii) A second order approach, by means of curvature estimates of the image curves at $\mathbf{x}_{i_o}$, can be used. The basic equations have been derived in [1] although further theoretical and experimental investigation is needed.

3.4 Special cases: sphere and cylinder

Let us assume that we have some a priori information about the surface. Such information may be translated into a relationship $R(a, b, c) = 0$ between the second order surface parameters. $R(a, b, c) = 0$ can be seen as a surface (or a volume or a curve, depending on the type of relationship) in the space of paraboloids. Thus, by intersecting the family (line) γ and such $R(a, b, c) = 0$, more information about the mirror surface become available. In some particular cases, the full second order surface description can achieved. Let us examine two interesting cases.

Sphere. If the mirror surface is a sphere with unknown radius r, the relationship $R(a,b,c)=0$ becomes: $a=b$ and $c=0$, which is simply a line ρ lying in the plane defined by $c=0$. At $s=s^*$, the intersection between ρ and γ allows to compute r. Namely, imposing that $a=b$ and having in mind Eq. 17, we obtain:

$$k=\frac{J_u-Jv}{v_1-v_2}; \qquad r=\frac{2(v_1-v_2)\cos\theta}{J_v v_1-J_u v_2} \tag{18}$$

Eq. 18 completely solves the ambiguity of type I.

Additionally, by imposing that $c=0$, we have $k\, v_3/\cos\theta=0$. Since $\cos\theta\neq 0$ and $k\neq 0$ (otherwise the surface would be singular), v_3 must be zero, namely:

$$\phi(s^*)=-B_{v_i}B_{u_j}\tan\varphi_j+B_{u_i}B_{v_j}\tan\varphi_i=0 \tag{19}$$

which is exactly the result achieved in [1]: the parameter s^* was found by imposing $\phi(s)$ to vanish. The condition $\det(\mathbf{H}^T\mathbf{H})=0$ given in this paper is a generalization. Notice that $\phi(s)$ is the determinant of the 2×2 matrix $\mathbf{H}_s$ obtained by taking the i^{th} and j^{th} rows and the first 2 columns of $\mathbf{H}$. Since Eq. 19 holds $\forall i,j$ with $i\neq j$, $\det(\mathbf{H}_s)=0\Rightarrow\det(\mathbf{H}^T\mathbf{H})=0$. Such a result can be used in order to easily remove ambiguities of type II. In fact, if there is an $\bar{s}$ such that $\psi(\bar{s})=0$ but $\phi(\bar{s})\neq 0$, $\bar{s}$ must be a ghost solution.

Cylinder. Let us focus our attention on the side surface M_c of the cylinder. The second order term of the Taylor expansion around any point $\in M_c$ of the surface Monge form attached to M_c is described by a parabolic paraboloid (see, for instance, [6]). Thus, $R(a,b,c)=0$ is $c^2=ab$, which is the locus depicted in figure 3. At $s=s^*$, the intersection between such locus and γ gives:

$$k=\frac{(J_v v_1+J_u v_2)\pm\sqrt{(J_v v_1+J_u v_2)^2-4(v_1v_2-v_3^2)J_uJ_v}}{2(v_1v_2-v_3^2)} \tag{20}$$

The corresponding a, b and c can be computed by means of Eq. 16 or Eq. 17.

3.5 The reconstruction procedure for a generic smooth surface

According to the results discussed in previous sections, we outline the following reconstruction procedure. A calibrated camera facing an unknown mirror surface and a calibrated pattern (e.g. 3 lines intersecting in $\mathbf{x}_{p_o}$) are considered. The image point $\mathbf{x}_{i_o}$ and the tangent vectors of the image reflected curves at $\mathbf{x}_{i_o}$ are measured. Thus, the entries of $\mathbf{H}$ are function of s only (Eq. 15). Since $\det(\mathbf{H})(s)$ vanishes in s^*, where s^* is the correct distance between $\mathbf{O}_c$ and the reflection point $\mathbf{x}_{m_o}$, we solve $\det(\mathbf{H})(s)=0$ numerically. If s^* is the unique solution, $\mathbf{x}_{m_o}$ and the normal of the surface at $\mathbf{x}_{m_o}$ are calculated in s^* by means of Eq. 1 and Eq. 2. Thus, the first order description of the surface is completely known. As for the second order description, the parameters a, b and c, up to the unknown parameter k, are calculated by means of Eq. 16. If $\det(\mathbf{H})(s)=0$ yields multiple solutions, we may want to consider the discussion in 3.3.

4 Experimental results

Our setup is sketched in Fig. 2. A camera faces the mirror surface and the pattern. In our experiments, a Canon G1 digital camera, with image resolution of 2048×1536 pixels, was used. The surface was typically placed at a distance of $30 \div 50$ cm from the camera. The pattern — a set of planar triplets of intersecting lines — is formed by a tessellation of black and white equilateral triangles. For instance, 3 white dashed edges as in Fig. 5 form a triplet of lines. The camera and the ground plane (i.e. the plane where the pattern lies) were calibrated by means of standard calibration techniques.

The reconstruction routine proceeds as follows. We manually selected a pair of triplet of lines (i.e. a triplet of pattern lines and a corresponding triplet of reflected pattern lines) from the image plane. See, for instance, the 2 dashed line triplets in Fig. 5. The selected triangle edges were estimated with sub-pixel accuracy and a B-spline was used to fit the edge points. The points $\mathbf{x}_{p_o}$ and $\mathbf{x}_{i_o}$ were computed by intersecting the corresponding splines. The tangents at $\mathbf{x}_{p_o}$ and $\mathbf{x}_{i_o}$ are obtained by numerically differentiating the splines. According to Sec. 3, $\mathbf{x}_{p_o}$, $\mathbf{x}_{i_o}$ and the corresponding tangents are used to estimate the distance s from the reflection point $\mathbf{x}_{m_o}$ on mirror surface to the center of the camera. The normal of the surface and the tangent plane at $\mathbf{x}_{m_o}$ are estimated by means of Eq. 2. We validated the method with four mirror surfaces: a plane (Fig. 5), a sphere (Fig. 6), a cylinder (Fig. 7) and a sauce pan's lid (Fig. 9) . Where we had a ground truth to compare with, we qualitatively tested the reconstruction results. As for the plane, depth and normal reconstruction errors are about 0.2% and less than 0.1% respectively. As for the sphere, the curvature reconstruction error is about 2%.

As explained in more details in [1], the reconstruction is not feasible when a pattern line is either orthogonal or belonging to the principal plane. In such cases, the constraint expressed by the tangent vector does no longer carry meaningful information. See Fig. 7 for an example. As a further remark, according to Sec. 3.3, we remind that each reconstructed point might be associated to one or more ghost solutions. Such solutions were easily rejected since always located farther than the correct ones from the center of camera . See Fig. 7 for examples.

From a practical point of view, detection and labeling of reflected and pattern lines are not to be considered a negligible issue. We notice here that in presence of unpolished mirror surfaces, the lines and the corresponding tangents might be estimated with a certain amount of noise. Further work is needed to study how much such a noise may affect the reconstruction results. It might also be interesting to relate the tangent estimate accuracy to the surface local curvature. Additionally, notice that we have always considered smooth surfaces. Since the analysis is local, the smoothness is not a necessary hypothesis for the reconstruction to be feasible as long as the reflecting points do not lie in any surface discontinuities. However, in practice, reflected pattern lines may be very hard to detect in a neighborhood of the discontinuities. This is also the case when concave surfaces are considered: although (as discussed in Sec. 2) the method

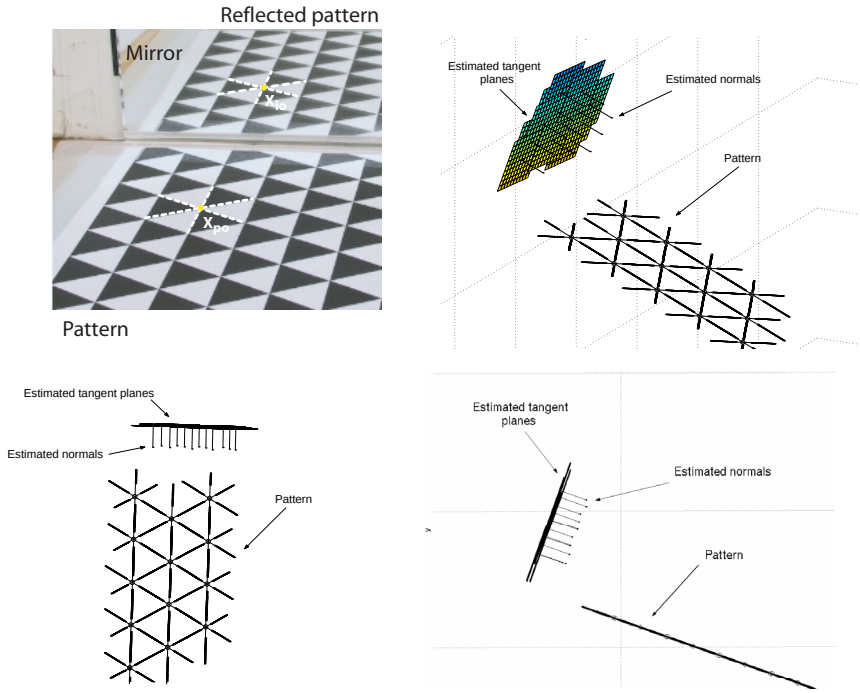

Fig. 5. Reconstruction of a planar mirror. Upper left panel: a planar mirror placed orthogonal with respect to the ground plane. A triplet of pattern lines and the corresponding reflected triplet are highlighted with dashed lines. We calculated the ground truth on the position and orientation of the mirror by attaching a calibrated pattern to its surface. We then reconstructed 15 surface points and normals with our method. The resulting mean position error (computed as average distance from the reconstructed points to the ground truth plane) is -0.048 cm with a standard deviation of 0.115 cm. The mean normal error (computed as the angle between ground truth plane normal and estimated normal) is 1.5×10^{-4}rad with a standard deviation of 6.5×10^{-4}rad. The reconstructed region is located at about 50 cm to the camera. **Upper right:** 3/4 view of the reconstruction. For each reconstructed point, the normal and the tangent plane are also plotted. **Lower left:** top view. **Lower right:** side view.

deals with generic surfaces, multiple reflections and inter-reflections can make the line detection a quite difficult problem.

5 Conclusion and future work

We have presented an explicit solution for reconstructing the first order local geometry (position and normals) of generic smooth mirror surfaces. Such analysis

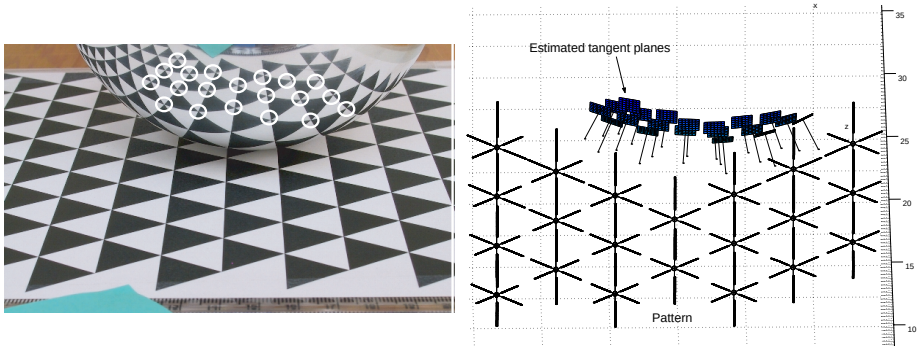

Fig. 6. Reconstruction of the sphere. Left panel: a spherical mirror with radius $r = 6.5$ cm, placed on the ground plane. We reconstructed the surface at the points highlighted with white circles. For each surface surface point we estimated the radius by means of Eq. 18. The mean reconstructed radius is 6.83 cm and the standard deviation is 0.7 cm. The reconstructed region is located at a distance about 30 cm to the camera. **Right panel:** top view of the reconstruction.

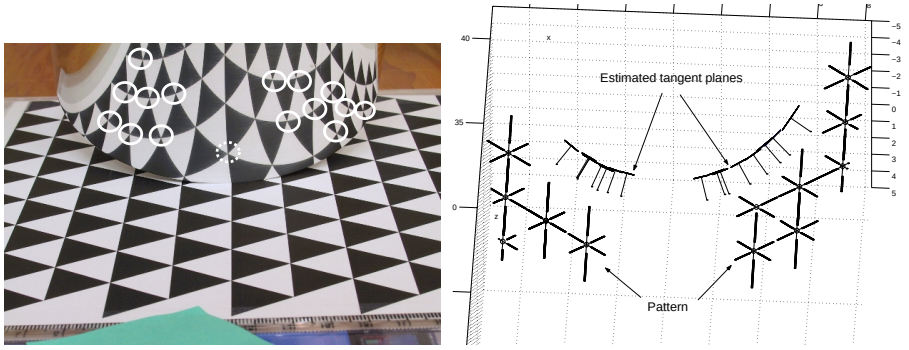

Fig. 7. Reconstruction of the cylinder. Left panel: a cylinder placed with the main axis almost orthogonal to the ground plane. We reconstructed the surface at the points highlighted with white circles. The dashed circle indicate an instance of point for which the reconstruction is not feasible or highly inaccurate (see Sec. 4). **Right:** top view of the reconstruction.

relates the position of a point in the image, and the orientation of 3 lines through that point, to the local structure of the mirror around the point of reflection. A few discrete ambiguities in the reconstruction may arise. They may be removed by considering either more than 3 no-coplanar lines or a rough a priori estimate of the surface point location. Additionally, we have explicitly expressed the second

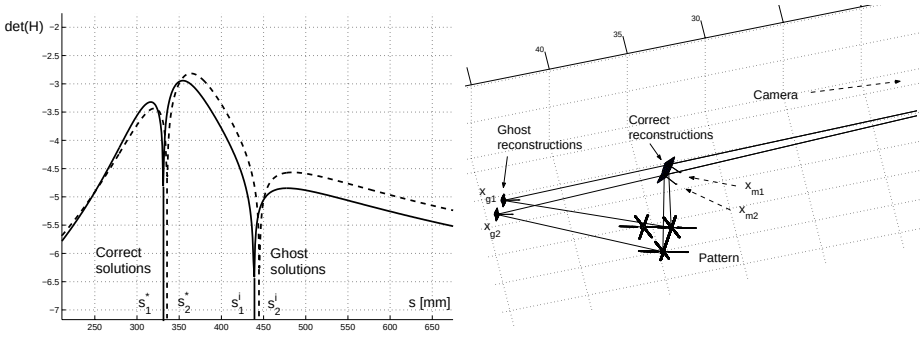

Fig. 8. Example of ambiguities of type II. Left panel: Two reconstructed points from the cylinder are considered. The plots of the corresponding det(**H**) functions are in dashed and solid lines. The corresponding correct solutions are s_1^* and s_2^*. The ghost solutions are s_1' and s_2' respectively. **Right:** The correct reconstructed points (attached to s_1^* and s_2^*) are $\mathbf{x}_{m_1}$ and $\mathbf{x}_{m_2}$. The ghost solutions are $\mathbf{x}_{g_1}$ and $\mathbf{x}_{g_2}$. Such solutions can be easily rejected since they appear at about 10 cm farther than the correct ones.

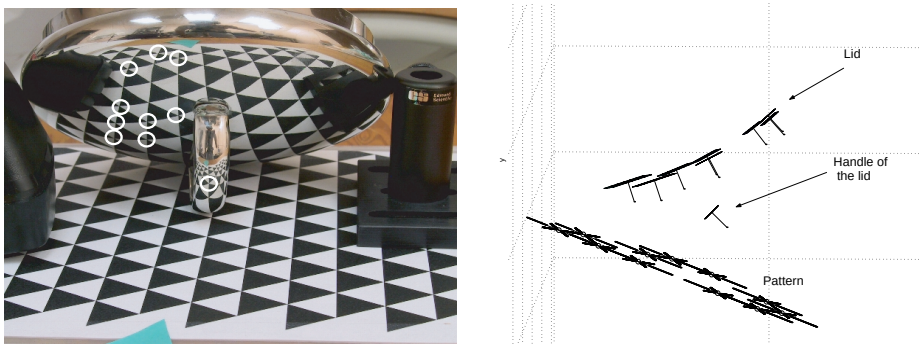

Fig. 9. Reconstruction of the sauce pan's lid. Left panel: a sauce pan's lid placed with the handle touching the ground plane. We reconstructed the surface at the points highlighted with white circles. Notice that one point belongs to the handle of the lid. **Right panel:** side view of the reconstruction. Notice how the reconstructed point on the handle sticks out from the body of the lid.

order local surface parameters as a function of an unknown scalar factor. Finally, we have validated our analysis with experimental results.

Future work is needed to study how sensitive the estimated parameters are with respect to noise added to the tangents, to investigate whether the second order ambiguity can be solved by measuring the reflected line curvatures or whether such ambiguities would disappear if the pattern is differentially moved in a known direction, and, finally, to extend the analysis to the stereoscopic vision case.

We view our results as a promising start in the quest of computing the global shape of specular surfaces under fairly general conditions. The more interesting case of an uncalibrated world appears much more challenging and will require most certainly the integration of additional cues and some form of prior knowledge on the likely statistics of the scene geometry.

6 Acknowledgments

This work is supported by the NSF Engineering Research Center for Neuromorphic Systems Engineering (CNSE) at Caltech (EEC-9402726). We wish to thank Min Chen, Marzia Polito and Fei Fei Li for helpful feedback and comments.

References

1. S. Savarese and P. Perona: Local Analysis for 3D Reconstruction of Specular Surfaces. *IEEE Conf. on Computer Vision and Pattern Recognition*, II 738–745 (2001)
2. T. Binford: Inferring surfaces from images. *Artificial Intelligence*, **17** (1981) 205–244.
3. A. Blake: Specular stereo. *IJCAI* (1985) 973–976.
4. A. Blake and G. Brelstaff: Geometry from specularities. *ICCV Proc. of Int Conf. of Computer Vision* (1988) 394–403.
5. M. Chen and J. Arvo: Theory and Application of Specular Path Perturbation. *ACM Transactions on Graphics.* **19** (2000) 246–278.
6. R. Cipolla and P. Giblin: Visual motion of curves and surfaces. *Cambridge University Press* 2000.
7. M. Halsead, A. Barsky, S. Klein, and R. Mandell: Reconstructing curved surfaces from reflection patterns using spline surface fitting normals. *SIGGRAPH* (1996).
8. G. Healey and T. Binford: Local shape from specularity. *Computer Vision, Graphics, and Image Processing* **42** (1988) 62–86.
9. K. Ikeuchi: Determining surface orientation of specular surfaces by using the photometric stereo method. *IEEE PAMI* **3** (1981) 661–669.
10. J. Koenderink and A. van Doorn: Photometric invariants related to solid shape. *Optica Apta* **27** (1980) 981–996.
11. M. Oren and S. K.Nayar: A theory of specular surface geometry. *Trans. Int. Journal of Computer Vision* (1997) 105–124.
12. J. Zheng and A. Murata: Acquiring a complete 3d model from specular motion under the illumination of circular-shaped light sources. *IEEE PAMI* **8** (2000).
13. A. Zisserman, P. Giblin, and A. Blake: The information available to a moving observer from specularities.*Image and Video Computing* **7** (1989) 38–42.
14. D. Perard: Automated visual inspection of specular surfaces with structured-lighting reflection techniques. *PhD Thesis – VDI Verlag* **Nr. 869** (2001)